

Conductive Polymer/SiO₂ Composite as an Anticorrosive Coating Against Carbon Dioxide Corrosion of Mild Steel. A Simulation Study.

K. Avchukir* and B.D. Burkitbayeva

Center of Physical Chemical Methods of Research and Analysis, al-Farabi Kazakh National University,
96a Tole bi str., Almaty, Kazakhstan

Article info

Received:
12 February 2020

Received in revised form:
27 April 2020

Accepted:
16 June 2020

Keywords:

Mild steel
Carbon dioxide corrosion
Polypyrrole
Silicon dioxide
Corrosion simulation

Abstract

In this work corrosion of mild steel affected by carbon dioxide was studied using a simulation model developed by Nordsveen M. and Nescic S. Using this comprehensive model of the uniform corrosion made possible to predict of corrosion rate of steel in the carbonic acid medium and the influence of different conditions on the anticorrosive property of coated electrode has been investigated. 1D model of corrosion process includes Butler-Volmer and Tafel equations and takes into account both the kinetics of anodic dissolution of an iron and electrochemical discharge of carbonic acid, water and hydrogen ions. The model has been created in COMSOL Multiphysics software and further improvement of this model allowed studying the influence of parameters such as solution composition, the partial pressure of CO₂, temperature and flow velocity of the solution on the corrosion rate of the steel. The results of numerical simulation demonstrate that the use of conductive polymer-polypyrrole/SiO₂ composite as an anti-corrosive resin coating reduces the corrosion rate of mild steel by 7 times or more, depending on pH, temperature and flow rate. Furthermore, increasing of flow velocity from 0.1 to 10 m/s affects to the removal of corrosion products from the surface of mild steel and as a result corrosion rate raises from 0.3 to 0.45 mm/year at a temperature of 80 °C and pH=4.

1. Introduction

Corrosion of industrial metals is one of the actual problems faced by science owing to its disastrous impact on the environment. The corrosion causes economic loss and reduces the service life of the materials and as well as leads to their degradation. The carbonic acid solution is one of the common corrosive environments. Corrosion by carbon dioxide in the presence of dissolved substances is an important issue in oil transportation and its industry. The surface degradation rate caused by corrosion depends on numerous factors including pH of the solution, partial pressure of carbon dioxide gas, temperature, flow conditions and metal or alloy composition. Therefore, the development of models that would predict the corrosion rate under various conditions and, thus, save the cost of performing a series of experiments is relevant. In

*Corresponding author.

E-mail: khaisa.avchukir@cfhma.kz

consideration of the dependence of corrosion rate on concrete variables, the model should lend itself to extrapolation for each major factor. It can be solved by a comprehensive model that realistically addresses the electrochemical and chemical processes that occur on the surface of corroding metal.

A model of uniform carbon dioxide corrosion of mild steel (MS) has been developed by several researchers [1–4] in the form of electrochemical models for surface processes or semi-empirical correlations. A major issue for model development has been the effect of insoluble corrosion products on corrosion rate, for example, an iron carbonate [5]. The experimental investigations, in the case of studying the electrochemical behaviour of carbon dioxide corrosion, have been performed by numerous authors [6–15]. Therefore, there is a need for developing a model that would simulate corrosion mild steel/conductive polymer/metal oxides or another doping agent composite electrode in CO₂, H₂S containing solutions including iron carbonate effect.

Organic coatings, particularly conductive polymers are intensively applied for the corrosion protection of steel due to their flexibility, ability to protect against surface degradation in a different aggressive environment and comparatively low cost. Ability to electrochemical synthesis owing to its relatively high conductivity, ease of electrochemical polymerization and good adhesion nature make conductive polymers and composites on its base appropriate candidate to be used as a coating for corrosion protection [16–21]. For example, one of the comprehensively investigated conductive polymers – polypyrrole (PPy) has a list of important properties such as good electrical conductivity, mechanical and environmental stability for corrosion protection application. Significant progress has been made in the past twenty years toward the application of polypyrrole on corrosion protection of industrial metals [22]. There are lots of traditional ways of protection against degradation of surface; they are based on different mechanisms such as sacrificial protection, barrier-like and active mechanism (for example, using corrosion inhibitors). The combination of active corrosion protection offered by conductive polymer with the passive protection imparted by the inorganic oxide filler would increase the corrosion resistance by several orders of magnitude inspiring hope effectively and shortly.

The influence of different doping agents such as ZnO, TiO₂, Al₂O₃ and SiO₂ on corrosion rate due to increasing polarization resistance and enhancing mechanical properties have been investigated in numerous works [23, 24]. Above mentioned fillers improve the corrosion resistance of composite coatings by reinforcing polymer matrix against diffusion of electroactive species in aggressive medium. Literature analysis suggests that SiO₂ filling within the polymer matrix gives many advantages such as good adhesion, cross-linking, high corrosion and diffusion resistance of the coatings [22, 25–27]. Also, the PPy/SiO₂ composite differs with its economic effectiveness, eco-friendly property and high anti corrosivity.

Additionally, the simulation model should describe the full chemical processes including electrochemical reactions that occur in the aqueous media on the electrode surface (MS/PPy-SiO₂).

In this case, the model should combine the electrochemical reaction module with hydrodynamic conditions. It means that a chemical part is responsible for the prediction activities of all species and phase equilibrium in the solution. The hydrody-

amic module was applied for studying mass transport, flow velocity effect on corrosion rate by using the following parameters as diffusion coefficient of species, the viscosity of the solution, the thickness of hydrodynamic and diffusion layer. The electrochemical module of COMSOL Multiphysics software was used for computing the corrosion rate in acidic solution based on the kinetics of electrode processes occur on anode and cathode part of steel surface by taking into account solution composition and flow conditions. Thus, the objective of this work includes the prediction of the corrosion rate of steel electrode in carbon dioxide containing an acidic aqueous solution using earlier developed models and its further enhancement.

2. Theory and mathematical model

A model of low carbon steel corrosion which had been used in this work allows computing the corrosion rate at different conditions. The model has been created on the base of models developed by Nordsveen [2] and Nescic and others [1]. Further enhancement of this model has been done by appending hydrodynamic condition as a turbulent flow of carbon dioxide to the surface of the steel electrode.

In this model corrosion process on a mild steel pipe surface at a turbulent flow condition has been simulated. In order to simplify the computation 1D model was chosen which includes processes taking place between the steel surface and depth of the solution. Since the model is one-dimensional, this implies that possible deviations along the length of the pipe cannot be taken into account. Additionally, the interaction of the gas-solution mixture with the mild steel pipe is confined to the near-electrode (surface) boundary layer. The thickness of the boundary layer depends on the hydrodynamic condition characterized by Reynolds number [28]. The structure of above mentioned boundary layer – geometry of the model and its physical considerations are shown in Fig. 1.

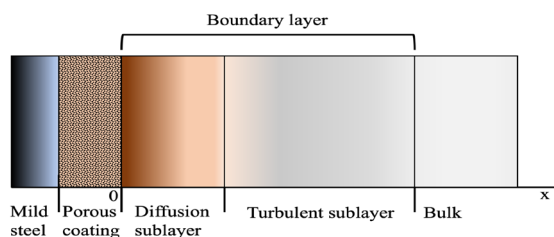


Fig. 1. The scheme of the boundary layer of the mild steel electrode; the description of geometry of 1D model. The porous coating consists of iron carbonate and SiO₂ doped PPy layer.

The diffusion and turbulent sublayers depend on mass transport parameters and they have been varied. The model was created by using the Corrosion

interface of COMSOL Multiphysics 5.4 software. The parameters used in this numerical simulation are shown in Table.

Table
Parameters used in the simulation model

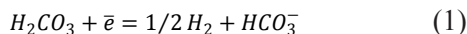
Parameter	Description
$d = 0.015 \text{ m}$	Pipe diameter
$\rho_{Fe} = 7850 \text{ kg/m}^3$	Density of steel
Electrolyte	
$\mu = 1.002 \times 10^{-3} \text{ kg/(m} \cdot \text{s)}$	Viscosity (at T=293.15 K)
$\rho = 997.7 \text{ kg/m}^3$	Density
0.185	Ionic strength in molar
$p_{CO_2} = 1$	Partial pressure of CO_2 in bar
$C_{CO_2} = 38.7 \text{ mol/m}^3$	Initial concentration of CO_2 (at $p_{CO_2} = 1 \text{ bar}$)
4-6	pH
Thermodynamic parameters	
$E = -0.488 \text{ V}$	Reversible potential for Fe oxidation
This parameters depend on pH, T and p_{CO_2} and were calculated according to Nernst equation	Reversible potential for H^+ reduction
	Reversible potential for H_2CO_3 reduction
	Reversible potential for water reduction
Kinetic parameters	
$j_0 = 0.05 \text{ A/m}^2$	Exchange current density for H^+ reduction
$j_0 = 0.06 \text{ A/m}^2$	Exchange current density for H_2CO_3 reduction
$j_0 = 3 \times 10^{-5} \text{ A/m}^2$	Exchange current density for water reduction
$j_0 = 2 \times 10^{-6} \text{ A/m}^2$	Exchange current density for Fe oxidation (values of j_0 for MS/PPy and MS/PPy/SiO ₂ electrodes were calculated using polarization resistance magnitudes from works [27, 30])
$j_{l_{H_2}} = -nFk_{m_{H^+}}C_{H^+}$	Limiting current density of hydrogen evolution reaction
$b_{H_2} = 0.118 \text{ V}$	Tafel slope for H^+ reduction
$b_{H_2CO_3} = 0.120 \text{ V}$	Tafel slope for H_2CO_3 reduction
$b_{H_2O} = 0.118 \text{ V}$	Tafel slope for water reduction
$b_{Fe} = 0.040 \text{ V}$	Tafel slope for Fe oxidation
Mass transfer parameters	
$D_{CO_2} = 1.96 \times 10^{-9} \text{ m}^2/\text{s}$	Diffusion coefficient of CO_2
$D_{H_2CO_3} = 2.0 \times 10^{-9} \text{ m}^2/\text{s}$	Diffusion coefficient of H_2CO_3
$D_{HCO_3^-} = 1.11 \times 10^{-9} \text{ m}^2/\text{s}$	Diffusion coefficient of HCO_3^- ions
$D_{CO_3^{2-}} = 9.2 \times 10^{-10} \text{ m}^2/\text{s}$	Diffusion coefficient of CO_3^{2-} ions
$D_{H^+} = 9.31 \times 10^{-9} \text{ m}^2/\text{s}$	Diffusion coefficient of H^+ ions
$D_{OH^-} = 5.26 \times 10^{-9} \text{ m}^2/\text{s}$	Diffusion coefficient of OH^- ions
$D_{Fe^{2+}} = 7.2 \times 10^{-10} \text{ m}^2/\text{s}$	Diffusion coefficient of Fe^{2+} ions
$k_{m_{H^+}} = D_{H^+}/d \times 0.0165 \times Re^{0.86} \times Sc_{H^+}^{0.33}$	Mass transfer coefficient for H^+
$Sc_{H^+} = \mu/\rho D_{H^+}$	Schmidt number for H ⁺
Hydrodynamic parameters	
$v = 0.1 - 10 \text{ m/s}$	Flow velocity
$Re = dv\rho/\mu$	Reynold's number
$\delta = 25 \times Re^{-7d/8}$	Boundary layer thickness

In addition, expect the parameters which are shown in Table also parameters such as Henry's constant, the equilibrium constant of CO₂ hydration, H₂CO₃ dissociation, HCO₃⁻ dissociation, water dissociation reactions required in this numerical simulation were taken from the literature [1–4]. Also, the initial concentration of all species in solution (CO₂, H₂CO₃, HCO₃⁻, CO₃²⁻, H⁺, OH⁻, Fe²⁺) was calculated using the above mentioned equilibrium constants.

The mass transport process including migration, diffusion and convection parts were modeled separately, but in all case species in the solution are assumed as diluted. Carbon dioxide hydration, water dissociation, proton, water and carbonic acid reduction reactions, and iron dissolution reaction are accounted for resulting in above mentioned seven species in the model. The simulation model takes into account electrochemical reactions that occur on the metal surface and transport processes for the species participating in reactions. Additionally, the model combines the partial cathodic and anodic processes to compute corrosion rates in the framework of the mixed potential theory.

On the mild steel surface, the current density is determined by the electrochemical reaction rate. In this model, three cathodic reactions are considered. One is the electrochemical reduction of carbonic acid, contributing to the hydrogen accumulation on the surface of MS; the other is the evolution of hydrogen from proton or water molecule depending on pH, competing with carbonic acid reduction.

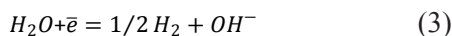
Carbonic acid reduction:



Proton reduction:



Water reduction:



The reaction rate of above-mentioned cathodic reactions depends not only on the electrode potential but also on the surface concentration of H₂CO₃, H⁺ species. The current density resulted from proton reduction can be expressed by the concentration dependent Butler-Volmer equation:

$$i_{(H^+)} = i_{0(H^+)} \times \left\{ \frac{[H^+]_s}{[H^+]_b} \times e^{\left(-\frac{\alpha_c F}{RT} \eta\right)} \right\}$$

where $i_{0(H^+)}$ and α_c are the exchange current density and transfer coefficient of H⁺ ion reduction, T is the temperature, R is the universal gas constant, η is the overpotential, $[H^+]_s$ and $[H^+]_b$ are the surface

and bulk equilibrium concentration hydrogen ions, respectively.

Since water is solvent, it can be assumed that the reduction rate of H₂O (depending on pH) is controlled by the charge-transfer process and, hence, pure Tafel behavior [1]:

$$i_{(H_2O)} = i_{0(H_2O)} \times 10^{-\frac{\eta}{b_c}}$$

where $i_{0(H_2O)}$ is exchange current density of water reduction reaction, b_c – cathodic Tafel slope.

Similarly, the kinetics of carbonic acid reduction should be represented as:

$$i_{(H_2CO_3)} = i_{0(H_2CO_3)} \times 10^{-\frac{\eta}{b_c}}$$

The total cathodic current density determines one of the boundary condition of the electrolyte:

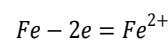
$$i_c = i_{(H^+)} + i_{(H_2O)} + i_{(H_2CO_3)}$$

In the present model, the corrosion of mild steel was taken the anodic dissolution of iron at the corrosion potential (and up to 100 mV above) was under activation control. Thus, pure Tafel behavior can be assumed close to the corrosion potential [1]:

$$i_{(Fe)} = i_{0(Fe)} \times 10^{\frac{\eta}{b_a}}$$

where $i_{0(Fe)}$ is exchange current density of iron dissolution reaction, b_a – anodic Tafel slope.

In this case, the total current density on the anode is related to the iron dissolution reaction:



The exchange current density for iron dissolution reaction on pure MS electrode, MS electrode coated with PPy and MS/PPy-SiO₂ composite electrodes were calculated from the magnitude of polarization resistance according to works [26, 29]. The turbulent sublayer has been modeled by adding a turbulent diffusivity term to the diffusion coefficient. The turbulent sublayer depends on the flow rate, viscosity, density of the liquid, and distance from the steel surface. The values of the diffusion coefficient of species and constants of equilibrium reactions were taken from works [1–4, 30, 31]. The mesh density in the vicinity of the boundaries was higher than that in the bulk region, facilitating the calculation of the high gradient conditions. The secondary current distribution interface of the Corrosion module of the COMSOL Multiphysics 5.4 software was used for solving this problem.

3. Results and discussion

The corrosion behavior of mild steel, MS coated with polypyrrole and MS coated with silica oxide doped polypyrrole layer in carbon dioxide-saturated mildly acidic solutions were investigated varying pH of the solution, temperature regime and flow velocity.

Figure 2 shows the concentration distribution of all species along with the boundary layer at 20 °C and pH 6. The concentration distribution curves demonstrate that the concentration of Fe^{2+} ions is significantly higher in the near-electrode layer due to the dissolution of steel electrode (a) and mild steel coated with polypyrrole (b), respectively. Also, a comparatively high concentration of hydrogen carbonate anion demonstrates significantly hydration of the carbon dioxide molecule at this condition.

Figure 2 demonstrates the absence of difference between concentration profile species on steel elec-

trode and steel electrode covered with polypyrrole. The reason for this is the high conductivity and low corrosion resistance of the pure polypyrrole layer. Covering of mild steel surface with PPy by electrochemical polymerization creates just a physical barrier between aggressive species and MS surface, but corrosion current decreases insignificantly. However, diffusion of a molecule of water and ions through PPy layer during the immersion of the electrode in solution leads to oxidizing of the metal surface and formation of corrosion products. These corrosion products could increase the conductive polymer film resistance by accumulating within the pores, this effect depends on immersion time and property of PPy film [25]. Since the corrosion current is also dependent from the temperature regime and pH of the solution, the influence of these factors on the corrosion rate had been studied.

Figure 3 shows the corrosion rate of the MS and MS/PPy surface at three different pH for operating temperatures ranging from 20 to 80 °C.

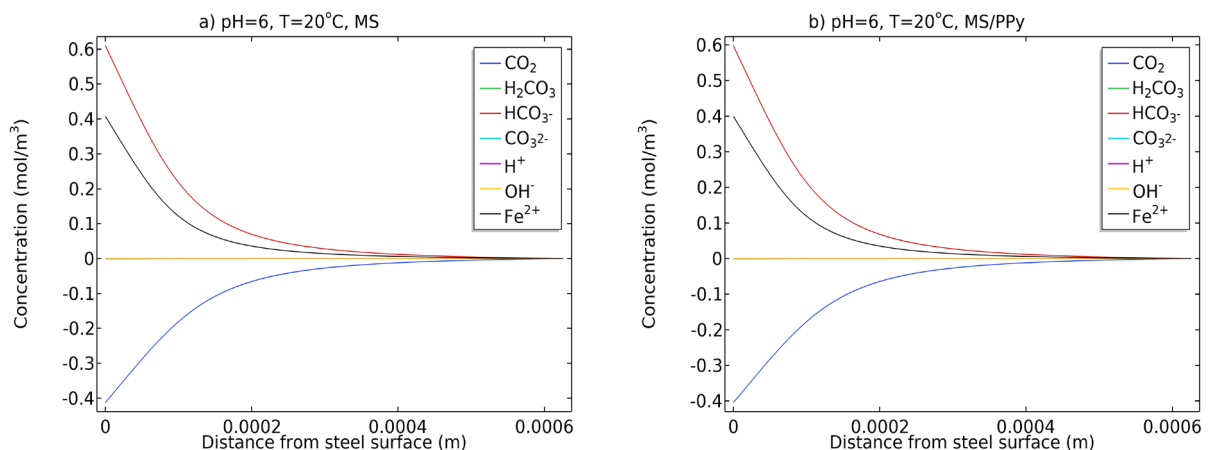


Fig. 2. The concentration distribution curve of species along the boundary layer of mild steel electrode during the corrosion process: a – on the MS electrode; b – on the MS/PPy electrode. Condition: pH = 6, T = 20 °C.

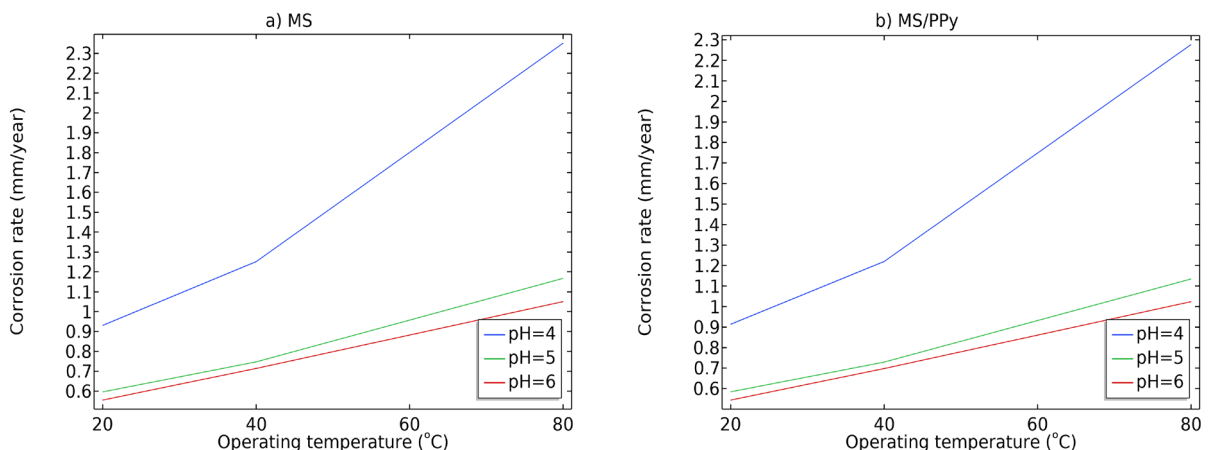


Fig. 3. The dependence of the computed value of corrosion rate in mm/year on temperature for pH of 4, 5 and 6, respectively: a – for the MS electrode; b – for the MS/PPy electrode.

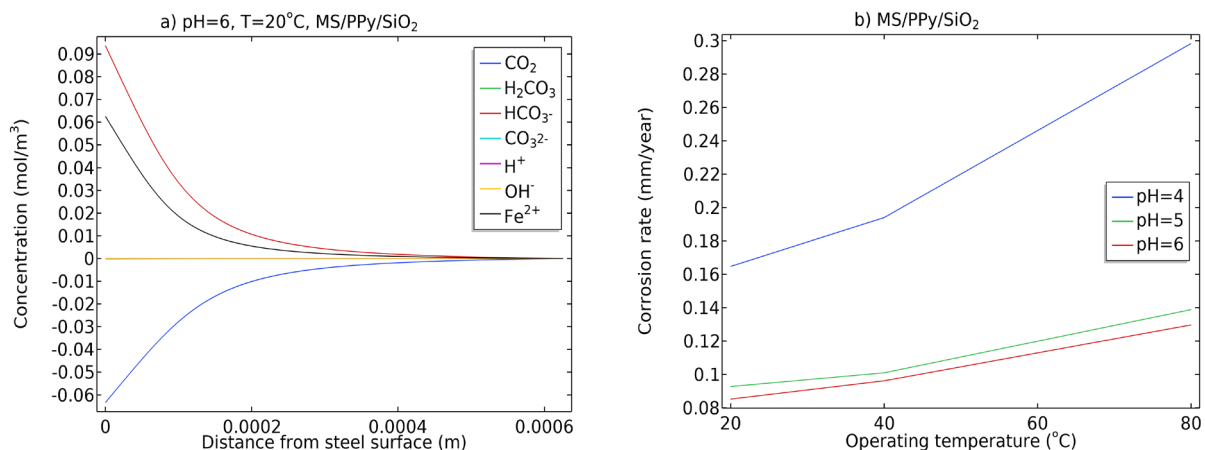


Fig. 4. a – The concentration distribution curve of species along the boundary layer of MS/PPy/SiO₂ composite electrode during the corrosion process; b – Corrosion rate of the MS/PPy/SiO₂ composite electrode in mm/year at different pH values and operating temperature range of 20–80 °C.

The corrosion rate of steel is directly proportional to the iron dissolution current since no other anodic reaction is considered. Lowered pH and increased temperature speed up the process and the corrosion rate of mild steel raised (Fig. 3). This suggests that polypyrrole coatings without any modifications do not provide a sufficient anti-corrosion effect.

One of the most efficient coating in term of corrosion protection is Steel/SiO₂/PPy film, probably as a consequence of more homogeneous doping of SiO₂ particles permitting a reasonable physical barrier effect [26]. In the references [25, 26] corrosion behavior of these composites was tested in 3.5% NaCl solution and the results of above mentioned investigations show a direct correlation between corrosion protection efficiency and percentage loading of polymer composite (SiO₂) in epoxy coating. In this work, the corrosion rate of the electrode coated with SiO₂/PPy composite in

an acidic carbon dioxide containing environment was predicted using numerical simulation technique (Fig. 4).

The results of the simulation demonstrated the using a conductive polymer-polypyrrole/SiO₂ composite as an anti-corrosive resin coating reduces the corrosion rate of mild steel by 7 times or more, depending on pH, temperature (Fig. 4). Also, Fig. 4 a shows that the concentration distribution of Fe²⁺ ions along near-electrode layer considerably smaller than on Steel/PPy surface and this explains the high protective effect of Steel/PPy/SiO₂ film.

The influence of the pH on the MS/PPy/SiO₂ composite electrode corrosion and concentration distribution of species during electrode degradation were investigated in a solution saturated with carbon dioxide, at electrolyte flow velocity equal to 0.1 m/s and operation temperature value 20 °C (Fig. 5).

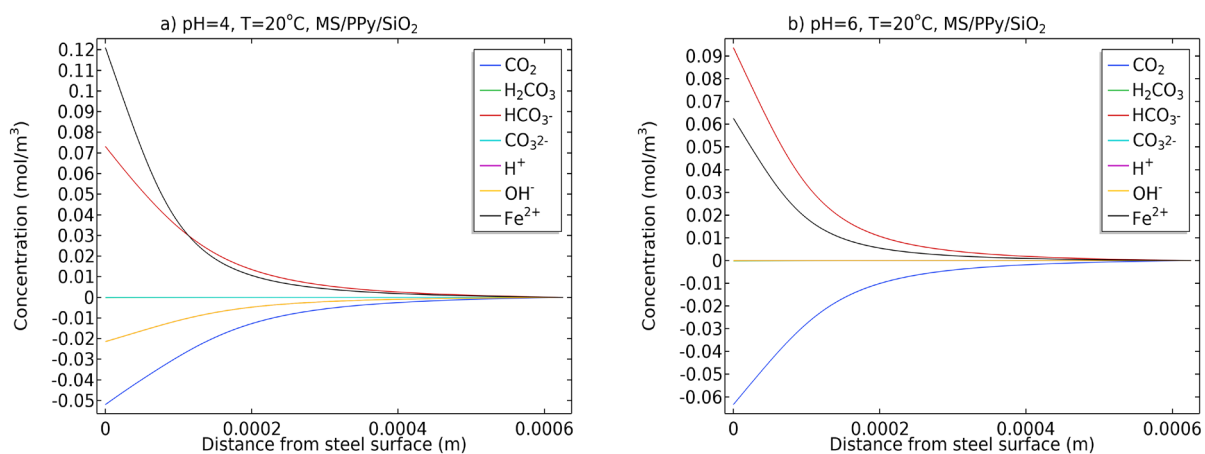


Fig. 5. The concentration distribution curve of species along the boundary layer of the MS electrode coated with PPy/SiO₂ composite at the temperature of 20 °C: a – pH=4; b – pH=6.

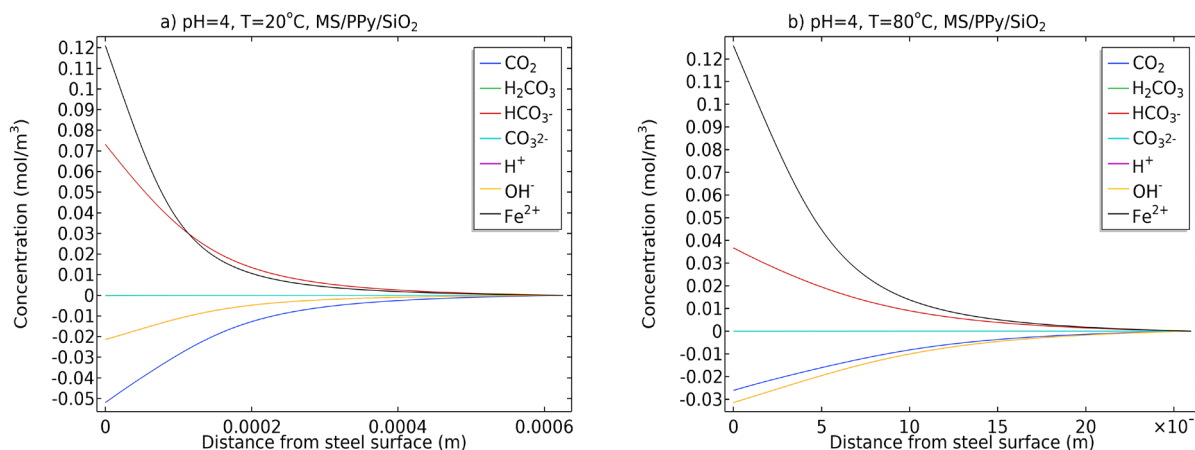


Fig. 6. The concentration distribution curve of species along the boundary layer of the MS electrode coated with PPy/SiO₂ composite in the solution with pH of 4 at different temperatures: a – 20 °C; b – 80 °C.

Comparison of the concentration profile of species during the MS/PPy/SiO₂ composite electrode corrosion show the direct correlation between the concentration of iron ions and pH. The decreasing of pH from 6 to 4 leads to increasing of Fe²⁺ ions (a product of corrosion) concentration on the boundary layer from 0.062 to 0.121 mol/l, respectively. However, in Fig. 5 b we can see the reverse effect on the concentration distribution curve of HCO₃⁻ anion. This effect should explain by the high intensity of carbonic acid reduction at pH=6 via reaction (1). In the case of pH range from 4 and below, the H⁺ reduction (reaction (2)) becomes the dominant cathodic reaction on the surface of the steel electrode as shown [2].

It is known that temperature accelerates both anodic and cathodic electrochemical processes upon the carbon dioxide corrosion of steel. As shown in Fig. 6, raising temperature results in an increased rate of limiting stage (charge transfer or mass transport) of electrode reaction and corrosion rate, respectively [30]. The effect of temperature on the kinetics of electrode reaction and equilibria of the carbon dioxide/water system well seen in Fig. 6b, as a result concentration of corrosion product (iron ions) increased in near-electrode layer.

In higher temperature conditions dissolution of iron, also the charge transfer processes are fast, as a consequence, the corrosion rate becomes under mass transfer control and the corrosion current is defined by the cathodic limiting current density. In this case, the mass transfer rate of H₂CO₃ and H⁺ species from the bulk becomes a determining component of limiting current. Obviously, it means that the changing of flow velocity influences the value of the limiting current density and as a result of corrosion rate, respectively. In the present mod-

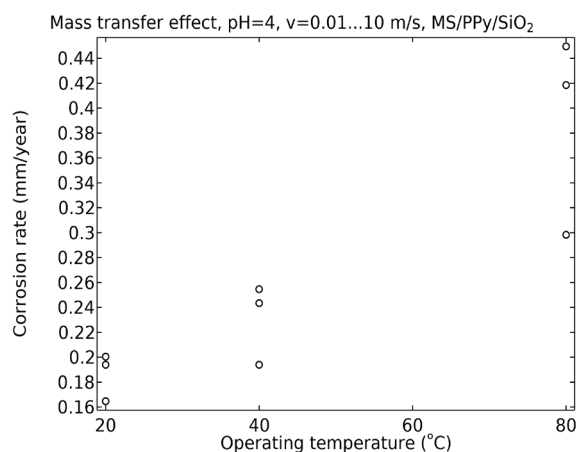


Fig. 7. The corrosion rate of MS/PPy/SiO₂ composite in mm/year for electrolyte flow rate range of 0.1–10 m/s at pH=4 and different operating temperatures: 20 °C, 40 °C, 80 °C.

el, the mass transfer in turbulent flow regimes is accounted for in terms of eddy diffusivity, as given [30].

The influence of the mass transport effect of aggressive species in the solution on the corrosion rate of MS/PPy/SiO₂ electrode was studied by varying flow rate velocity magnitude from 0.1 to 10 m/s. The dependence demonstrating flow rate velocity effect at comparatively low pH value (pH=4) for different values of temperature (20, 40, 80 °C) is given in Fig. 7.

According to Fig. 7, varying flow rate of electrolyte influences to corrosion rate of mild steel and this effect raises by increasing temperature. The increasing flow rate from 0.1 to 10 m/s affects the removal of corrosion products from the surface of mild steel and as a result corrosion rate raises from 0.3 to 0.45 mm/year at a temperature of 80 °C and pH=4. In addition, the flow rate effect is

pronounced at high temperature 80 °C, because at low temperatures role of activation barrier is high. At high temperature regime cathodic half-reaction becomes rate determining reaction, in this situation corrosion rate directly depends on mass transfer rate of H⁺ or H₂CO₃ species. According to equation of limiting current at stationary diffusion regime mass transfer coefficient directly proportional to convection speed. Mixing of solution (or rotating of electrode) with constant velocity forms hydrodynamic layer in near-electrode boundary layer is called Prandtl's layer with constant thickness. Effective thickness of diffusion layer which determines mass transfer rate of hydrogen ions approximately ten times smaller than Prandtl's layer thickness. Thickness of hydrodynamic layer depends on magnitude of flow velocity (in inverse ratio), hydrodynamic condition that could be explained using such parameters as Reynold's and Schmidt numbers shown in Table.

This study proposed a simple model of an uniform carbon dioxide corrosion of steel including fluid flow and mass transport but the effects of conductive polymer/silicon oxide layer degradation during the corrosion of the electrode surface were neglected. However, this simulation work can give useful information for mild steel corrosion prediction when a protective conductive polymer coating is employed.

4. Conclusion

A versatile one dimensional model of uniform corrosion of low carbon steel affected by carbon dioxide has been developed. The simulation model combines fluid dynamics calculations with electrochemical computations based on the mixed-potential theory. The electrochemical model takes into account the cathodic reduction of carbonic acid, proton, and water and the anodic dissolution process of the iron electrode, which may be under activation control. Also, the model includes the effects of a protective layer such as polypyrrole or hydrophobic polypyrrole layer filled with silicon oxide.

The simulation model of mild steel corrosion has been developed in COMSOL Multiphysics software that made it possible to study the effects of conditions such as electrolyte flow velocity, temperature, pH, and nature of a corrosion protection layer on average corrosion rate. The results of the simulation study show the reduction of pH of the solution raises the corrosion rate of mild steel. The influence of temperature on the corrosion rate

less noticeable at high pH area than low pH magnitude.

According to the results of electrolyte flow velocity varying experiment (computation), varying flow rate of electrolyte influences to corrosion rate of mild steel and this effect intensifies by increasing temperature. For example, the increase of average flow rate from 0.1 to 10 m/s affects the removal of corrosion products from the surface of mild steel and as a result corrosion rate raises from 0.19 to 0.25 mm/year at a temperature of 40 °C and pH=4.

Acknowledgement

The authors would like to thank the Ministry of Education and Science of the Republic of Kazakhstan, for its financial support (grant No. AP05134571-OT-19) of this study.

References

- [1]. S. Nestic, J. Postlethwaite, S. Olsen, *Corrosion* 52 (1996) 280–294. DOI: [10.5006/1.3293640](https://doi.org/10.5006/1.3293640)
- [2]. M. Nordsveen, S. Nešić, R. Nyborg, A. Stangeland, *Corrosion* 59 (2003) 443–456. DOI: [10.5006/1.3277576](https://doi.org/10.5006/1.3277576)
- [3]. S. Nešić, M. Nordsveen, R. Nyborg, A. Stangeland, *Corrosion* 59 (2003) 489–497. DOI: [10.5006/1.3277579](https://doi.org/10.5006/1.3277579)
- [4]. S. Nešić, K.-L.J. Lee, *Corrosion* 59 (2003) 616–628. DOI: [10.5006/1.3277592](https://doi.org/10.5006/1.3277592)
- [5]. R. Barker, I. Al Shaaili, R.A. De Motte, D. Burkle, T. Charpentier, S.M. Vargas, A. Neville, *Appl. Surf. Sci.* 469 (2019) 135–145. DOI: [10.1016/j.apsusc.2018.10.238](https://doi.org/10.1016/j.apsusc.2018.10.238)
- [6]. Q. Zhao, J. Guo, G. Cui, T. Han, Yanhua Wu, *Colloid. Surface. B* 194 (2020) 111150. DOI: [10.1016/j.colsurfb.2020.111150](https://doi.org/10.1016/j.colsurfb.2020.111150)
- [7]. M.A.J. Mazumder, H.A. Al-Muallem, M. Faiz, S.A. Ali, *Corros. Sci.* 87 (2014) 187–198. DOI: [10.1016/j.corsci.2014.06.026](https://doi.org/10.1016/j.corsci.2014.06.026)
- [8]. H. Mansoori, D. Young, B. Brown, M. Singer, *J. Nat. Gas Sci. Eng.* 59 (2018) 287–296. DOI: [10.1016/j.jngse.2018.08.025](https://doi.org/10.1016/j.jngse.2018.08.025)
- [9]. Yu.P. Khodyrev, E.S. Batyeva, E.K. Badeeva, E.V. Platova, L. Tiwari, O.G. Sinyashin, *Corros. Sci.* 53 (2011) 976–983. DOI: [10.1016/j.corsci.2010.11.030](https://doi.org/10.1016/j.corsci.2010.11.030)
- [10]. M.W.S. Jawich, G.A. Oweimreen, S.A. Ali, *Corros. Sci.* 65 (2012) 104–112. DOI: [10.1016/j.corsci.2012.08.001](https://doi.org/10.1016/j.corsci.2012.08.001)
- [11]. X. Guan, D. Zhang, J. Wang, Y. Jin, Y. Li, *J. Nat. Gas Sci. Eng.* 37 (2017) 199–216. DOI: [10.1016/j.jngse.2016.11.047](https://doi.org/10.1016/j.jngse.2016.11.047)

- [12]. Q.H. Zhang, B.S. Hou, N. Xu, H.F. Liu, G.A. Zhang, *J. Taiwan Inst. Chem. E* 96 (2019) 588–598. DOI: [10.1016/j.jtice.2018.11.022](https://doi.org/10.1016/j.jtice.2018.11.022)
- [13]. R. De Marco, Z.-T. Jiang, D. John, M. Sercombe, B. Kinsella, *Electrochim. Acta* 52 (2007) 3746–3750. DOI: [10.1016/j.electacta.2006.10.048](https://doi.org/10.1016/j.electacta.2006.10.048)
- [14]. A.A. Abd, S.Z. Naji, A.S. Hashim, *Eng. Fail. Anal.* 105 (2019) 638–646. DOI: [10.1016/j.engfailanal.2019.07.026](https://doi.org/10.1016/j.engfailanal.2019.07.026)
- [15]. I. Jevremović, M. Singer, S. Nešić, V. Misković-Stanković, *Corros. Sci.* 77 (2013) 265–272. DOI: [10.1016/j.corsci.2013.08.012](https://doi.org/10.1016/j.corsci.2013.08.012)
- [16]. D.E. Tallman, Y. Pae, G.P. Bierwagen, *Corrosion* 55 (1999) 779–786. DOI: [10.5006/1.3284033](https://doi.org/10.5006/1.3284033)
- [17]. P. Sambyal, G. Ruhi, R. Dhawan, S.K. Dhawan, *Surf. Coat. Tech.* 303 (2016) 362–371. DOI: [10.1016/j.surfcoat.2015.12.038](https://doi.org/10.1016/j.surfcoat.2015.12.038)
- [18]. G. Ruhi, O.P. Modi, S.K. Dhawan, *Synthetic Met.* 200 (2015) 24–39. DOI: [10.1016/j.synthmet.2014.12.019](https://doi.org/10.1016/j.synthmet.2014.12.019)
- [19]. P. Sambyal, G. Ruhi, S.K. Dhawan, B.M.S. Bisht, S.P. Gairola, *Prog. Org. Coat.* 119 (2018) 203–213. DOI: [10.1016/j.porgcoat.2018.02.014](https://doi.org/10.1016/j.porgcoat.2018.02.014)
- [20]. S.A. Kumar, H. Bhandari, C. Sharma, F. Khatoon, S.K. Dhawan, *Polym. Int.* 62 (2013) 1192–1201. DOI: [10.1002/pi.4406](https://doi.org/10.1002/pi.4406)
- [21]. J.P. Lu, L. Chen, R.G. Song, *Surf. Eng.* 35 (2019) 440–449. DOI: [10.1080/02670844.2018.1491511](https://doi.org/10.1080/02670844.2018.1491511)
- [22]. N. Jadhav, S. Kasisomayajula, V.J. Gelling, *Front. Mater.* 7 (2020). DOI: [10.3389/fmats.2020.00095](https://doi.org/10.3389/fmats.2020.00095)
- [23]. M. Mobin, R. Alam, J. Aslam, *J. Mater. Eng. Perform.* 25 (2016) 3017–3030. DOI: [10.1007/s11665-016-2145-x](https://doi.org/10.1007/s11665-016-2145-x)
- [24]. X. Shi, T.A. Nguyen, Z. Suo, Y. Liu, R. Avci, *Surf. Coat. Tech.* 204 (2009) 237–245. DOI: [10.1016/j.surfcoat.2009.06.048](https://doi.org/10.1016/j.surfcoat.2009.06.048)
- [25]. O. Grari, A.E. Taouil, L. Dhouibi, C.C. Buron, F. Lallemand, *Prog. Org. Coat.* 88 (2015) 48–53. DOI: [10.1016/j.porgcoat.2015.06.019](https://doi.org/10.1016/j.porgcoat.2015.06.019)
- [26]. G. Ruhi, H. Bhandari, S.K. Dhawan, *Prog. Org. Coat.* 77 (2014) 1484–1498. DOI: [10.1016/j.porgcoat.2014.04.013](https://doi.org/10.1016/j.porgcoat.2014.04.013)
- [27]. V.T.H. Van, T.T.X. Hang, P.T. Nam, N.T. Phuong, N.T. Thom, D. Devilliers, D.T.M. Thanh, *J. Nanosci. Nanotechnol.* 18 (2017) 4189–4195. DOI: [10.1166/jnn.2018.15198](https://doi.org/10.1166/jnn.2018.15198)
- [28]. COMSOL Myltiphysics, Carbon dioxide corrosion in steel pipes, (n.d.) 1–18. https://www.comsol.com/model/download/639711/models.corr.co2_corrosion.pdf
- [29]. A. Asan, G. Asan, *Journal of the Turkish Chemical Society Section B: Chemical Engineering* 2 (2019) 133–136.
- [30]. A. Kahyarian, S. Nesic, *Corros. Sci.* 173 (2020) 108719. DOI: [10.1016/j.corsci.2020.108719](https://doi.org/10.1016/j.corsci.2020.108719)
- [31]. A. Kahyarian, M. Singer, S. Nesic, *J. Nat. Gas Sci. Eng.* 29 (2016) 530–549. DOI: [10.1016/j.jngse.2015.12.052](https://doi.org/10.1016/j.jngse.2015.12.052)